

This work was written as part of one of the author's official duties as an Employee of the United States Government and is therefore a work of the United States Government. In accordance with 17 U.S.C. 105, no copyright protection is available for such works under U.S. Law.

Public Domain Mark 1.0

<https://creativecommons.org/publicdomain/mark/1.0/>

Access to this work was provided by the University of Maryland, Baltimore County (UMBC) ScholarWorks@UMBC digital repository on the Maryland Shared Open Access (MD-SOAR) platform.

Please provide feedback

Please support the ScholarWorks@UMBC repository by emailing scholarworks-group@umbc.edu and telling us what having access to this work means to you and why it's important to you. Thank you.

Non-self-similar scaling of plasma sheet and solar wind probability distribution functions of magnetic field fluctuations

J. M. Weygand,¹ M. G. Kivelson,¹ K. K. Khurana,¹ H. K. Schwarzl,¹ R. J. Walker,¹
A. Balogh,² L. M. Kistler,³ and M. L. Goldstein⁴

Received 28 April 2006; revised 3 August 2006; accepted 29 August 2006; published 9 November 2006.

[1] Solar wind magnetometer and plasma data and magnetometer data acquired by Cluster in the magnetospheric plasma sheet are employed to construct probability distribution functions (PDFs) of magnetic field fluctuations over various temporal and spatial scales. This technique, often used in analysis of laboratory plasmas, is used to look for intermittent plasma turbulence and non-self-similar properties in the fluctuations. We examine the distribution of the magnetic field fluctuations for a single spacecraft and between pairs of correlated spacecraft time series data in both the plasma sheet and the solar wind (fast and slow speed streams). We demonstrate that the plasma sheet fluctuations have a distribution consistent with intermittent turbulence and that they scale non-self-similarly using two different methods (Sorriso-Valvo et al., 1999; Hnat et al., 2002). In the solar wind both methods show that the fast solar wind magnetic field fluctuations have a PDF consistent with intermittent turbulence and scale non-self-similarly, but the two methods give conflicting results for the slow solar wind scaling properties. Finally, we use the results of the two methods as well as kurtosis versus scale size to roughly determine the turbulent eddy scale size in both types of solar wind (about 500 R_E) and the magnetospheric plasma sheet (between 0.9 and 1.5 R_E).

Citation: Weygand, J. M., M. G. Kivelson, K. K. Khurana, H. K. Schwarzl, R. J. Walker, A. Balogh, L. M. Kistler, and M. L. Goldstein (2006), Non-self-similar scaling of plasma sheet and solar wind probability distribution functions of magnetic field fluctuations, *J. Geophys. Res.*, *111*, A11209, doi:10.1029/2006JA011820.

1. Introduction

[2] Electromagnetic energy is stored in the magnetotail lobes and transferred to the plasma sheet and the most likely mechanism for this transport is reconnection. Reconnection produces flows and magnetic field fluctuations that appear to be turbulent. Understanding if these fluctuations are turbulent is important for understanding the physics of the plasma sheet. However, measurements to characterize spatial and temporal variations independently and to ascertain the role of PS turbulence in energy transport remain incomplete.

1.1. Probability Distribution Functions of Solar Wind Turbulence

[3] The presence of turbulence in the solar wind has been established by using different methods, some of which analyze probability distribution functions (PDFs) of flow and magnetic field fluctuations [Marsch and Tu, 1994; Sorriso-Valvo et al., 1999, 2001]. Many of these methods

have been employed to demonstrate the presence of turbulent fluctuations in the magnetospheric plasma sheet [Angelopoulos et al., 1999; Borovsky et al., 1997; Weygand et al., 2005]. Qualitatively, the PDFs in turbulent plasma are approximately Gaussian at large scales and become increasingly peaked, with high probability of large fluctuations in the wings at smaller scales. In terms of the kurtosis, which is the fourth moment of the distribution, the PDFs have a large kurtosis (leptokurtic) at small scales, which is associated with intermittent turbulence [Angelopoulos et al., 1999] and become mesokurtic at large scales (i.e., their kurtosis approaches 3). Both Marsch and Tu [1994] and Sorriso-Valvo et al. [1999, 2001] demonstrated this variation of the PDFs with scale size using Helios data in the solar wind, which had a resolution of 81 s. The nonlinear variation of the PDF with scale size is associated with non-self-similar scaling related to turbulence and has been observed in turbulent fluid flows [Castaing et al., 1990].

[4] Sorriso-Valvo et al. [1999, 2001] quantified the change in the PDFs in the inertial range from 81 s to a few hours by fitting them with a model developed by Castaing et al. [1990] that demonstrates how model parameters vary with scale size. The Castaing et al. [1990] model was developed from the classical Kolmogorov's picture of turbulent energy cascade [Kolmogorov, 1941] and took into account that the energy transfer rate in the cascade at different scales is not strictly self-similar. Their model, which fitted a PDF of flow fluctuations $\delta\psi$ at a given scale

¹Institute of Geophysics and Planetary Physics, University of California, Los Angeles, California, USA.

²Imperial College of Science and Technology, London, UK.

³Institute for the Study of Earth, Oceans, and Space, University of New Hampshire, New Hampshire, USA.

⁴NASA Goddard Space Flight Center, Greenbelt, Maryland, USA.

τ , is a convolution of a Gaussian and a log-normal distribution or equivalently is the sum of weighted Gaussian distributions with a log-normal distribution as the weighting function:

$$\Pi_{\lambda}(d\Psi) = \frac{A(a_s)}{2\pi\lambda} \int_0^{+\infty} \exp \left[-\frac{(d\Psi)^2}{2\sigma^2} \left(1 + a_s \frac{d\Psi/\sigma}{1 + (d\Psi)^2/\sigma^2} \right) \right] \cdot \exp \left(-\frac{\ln^2(\sigma/\sigma_0)}{2\lambda^2} \right) \frac{d\sigma}{\sigma^2} \quad (1)$$

Here $A(a_s)$ is a normalization constant, a_s is a skewness factor to account for asymmetry, σ_0 is the most probable value of σ , λ is the width of the log-normal distribution, and σ is the standard deviation for a Gaussian distribution. The *Castaing et al.* [1990] model was first applied to high Reynolds number turbulent flow. PDFs of the flow fluctuations varied from peaked distributions with high probabilities in the wings at relatively small spatial separations to more Gaussian distributions at larger spatial separations. *Castaing et al.* [1990] were able to fit the distributions qualitatively out to about 10 standard deviations.

[5] Using an approach similar to that of *Sorriso-Valvo et al.* [1999], *Burlaga and Viñas* [2004] examined the variation in the PDFs of the ACE plasma flow data at a resolution of 1 hour. The findings of their study were similar to those of *Sorriso-Valvo et al.* [1999], but *Burlaga and Viñas* extended the range of temporal separations to days. They showed that with increasing scale size, the PDFs become Gaussian at temporal separations of about 280 hours. The difference in the results appears to be related to the resolution of the data and the two studies are most likely characterizing different phenomena at different scales.

[6] *Leubner and Vörös* [2005] also examined PDFs constructed from solar wind magnetic field and flow as well as the density for a single spacecraft with data from the Wind and the ACE spacecraft. Their study shows that PDFs of the magnetic field, flow, and density become nearly Gaussian at large temporal separations. In particular for the magnetic field PDFs the PDFs were Gaussian for the Wind spacecraft for time differences of about 23 hours and about 44 hours for the ACE magnetic field PDFs. However, the exact separation at which this occurs was not determined.

[7] The fact that PDFs of fluctuations are non-Gaussian at small scales and do not scale self-similarly is thought to give evidence of intermittent turbulence. *Hnat et al.* [2002, 2003] took a different approach to the investigation of self-similarity. They examined the change of the PDFs peak versus the scale size and found that the scaling exponential is a non-linear function, hence the fluctuations are not self similar. However, they were able to linearly rescale the ion density, energy density B^2 and ρv^2 as well as the Poynting flux in the MHD limit.

1.2. PDFs of Plasma Sheet Turbulence

[8] Turbulence has been identified in the magnetospheric plasma sheet as well as in the solar wind. For plasma sheet studies different methods that have been used that include statistical examinations of PDFs of flow and magnetic field and the fluctuations of these quantities [*Borovsky et al.*,

1997; *Angelopoulos et al.*, 1999; *Petrukovich and Yermolaev*, 2002; *Weygand et al.*, 2005]. Most of these studies found non-Gaussian PDFs of flow and magnetic field fluctuations from which they concluded that the plasma was turbulent. In particular, *Borovsky et al.* [1997] examined the distribution of V_x and V_y flow observations made by ISEE-2 spacecraft during 10 plasma sheet traversals. The ISEE-2 two-dimensional Fast Plasma Analyzer did not regularly obtain the V_z component in the plasma distribution function. The distributions of the V_x and V_y components were well fit with an exponential function. *Borovsky et al.* attribute the high probability of flow values in the wings of the distribution (associated with bursty bulk flows (BBFs)) to eddy turbulence.

[9] The flow distributions were also analyzed by *Angelopoulos et al.* [1999] and *Petrukovich and Yermolaev* [2002]. *Angelopoulos et al.* [1999] examined the distribution of V_x and V_y components of the flow for BBFs, non-BBFs, and the combined data set using Geotail/LEP data. They did not analyze the V_z component of flow and it is not clear why not. In addition to showing the non-Gaussian shape of the distributions, *Angelopoulos et al.* [1999] fit the distributions with the *Castaing et al.* [1990] model. They found the model was a good fit for the distributions of the BBF flows and the non-BBF flows, but not for the distribution of the two combined. Using the CORALL instrument on the Interball Tail spacecraft, *Petrukovich and Yermolaev* [2002] examined the V_y and V_z flow components. The V_x component values were considered to be less accurate than the other two components because the ion flux measurements were not measured within $\pm 16^\circ$ of the Sun-pointing spin axis. This study did not attempt to fit the distributions to a model, but they found that the kurtoses of the distributions were greater than 9 for all components.

[10] Also of interest for this study is the *Angelopoulos et al.* [1999] observation of the non-Gaussian PDF of differences of V_y between two spatially separated spacecraft, Wind and Geotail. We believe this study is the first study in which two spacecraft were used to identify a non-Gaussian PDF. The statistics of two point measurements are a reliable indicator of turbulent fluctuations because turbulence relates to the structure of fluctuations in space. Single spacecraft measurements provide statistics of temporal fluctuations, which give information on spatial fluctuations if the Taylor hypothesis applies. The assumption is valid only if the fluctuations evolve slowly with respect to the time required for the plasma to flow past the spacecraft (i.e., the fluctuations must be frozen into the flow).

[11] As far as we are aware, only two studies have examined the scaling of PDFs of magnetic field fluctuations in the Earth's plasma sheet at inertial scales. *Weygand et al.* [2005] used a single Cluster spacecraft to demonstrate qualitatively the variation of the PDFs from a highly peaked PDF with large probabilities in the wings at small-scale sizes to Gaussian at large-scale sizes. They support their observations by demonstrating that the kurtosis systematically decreases with increasing scale size and by indicating that the PDFs cannot be linearly rescaled with the method introduced by *Hnat et al.* [2002]. *Consolini et al.* [2005] also employed a method similar to that of *Hnat et al.* [2002], but this study focused mostly on kinetics scales. They concluded that the PDFs of the magnetic field fluctu-

ations show non-Gaussian tails and at the kinetic scales the PDFs scale self-similarly in a way consistent with Lévy statistics. In the limited portion of the inertial range examined, which was from about the ion gyroperiod to periods of about 30 s, they determined that the fluctuations scale self-similarly in a manner consistent with classical Brownian motion. Similar results have been determined by Vörös *et al.* [2003, 2004], but, like the Consolini *et al.* [2005] study, these studies focus on the kinetic scales and the Vörös *et al.* studies use methods that employ multifractals and structure functions.

[12] In this study we use multiple spacecraft and two different analysis methods to show that the PDFs of the magnetic field fluctuations scale non-self-similarly over a range of temporal and spatial separations in both the fast solar wind and the plasma sheet. In section 2 we describe the data used in this study. In section 3 we outline the procedure for constructing PDFs from a single spacecraft and from spacecraft pairs and describe how the two types of PDFs can be compared. The Sorriso-Valvo *et al.* [1999] method of showing non-self-similarity is applied in section 4. In that section, we first follow previous investigators by using a single spacecraft to show non-self-similarity in the solar wind. Then we demonstrate that analogous results can be obtained with multiple spacecraft over a range of spatial separations. Finally we use the multispacecraft aspect of Cluster to show that non-self-similar scaling of PDFs is found within the plasma sheet under specific conditions. In section 5 we apply the method of Hnat *et al.* [2002] to demonstrate non-self-similar properties of the fast solar wind and the plasma sheet. This method shows that the slow solar wind has self-similar scaling properties, a result that conflicts with the results of Sorriso-Valvo *et al.* [1999]. Finally, in section 6, we discuss the similarities and differences between the results of this study and previous studies.

2. Data Sources

[13] Data from many spacecraft were used for this study. The magnetic field and plasma measurements within the plasma sheet were obtained from the Cluster spacecraft, the solar wind plasma and magnetic field data were obtained from the Advanced Composition Explorer (ACE), Cassini, Galileo, Geotail, IMP-8, and Wind. Cross-calibration has been undertaken for the four Cluster spacecraft instruments, but no such comparison has been applied to the instruments on the other spacecraft. Offsets that may exist among the instruments are small (i.e., a fraction of a nanoTesla) and are subtracted from the time series data during the data processing. These offsets are not significant to this study. The removal of the offsets does not change the results of this study.

[14] The Cluster mission, supported jointly by the European Space Agency (ESA) and NASA, consists of four identical spacecraft, optimally in a tetrahedral configuration, with a perigee of 4 R_E , an apogee of 19.6 R_E , and a spin period of 4 s. These four spacecraft are providing the first three-dimensional measurements of large- and small-scale phenomena in the near-Earth environment [Escoubet *et al.*, 1997]. Each Cluster spacecraft carries 11 instruments. This study uses data from the magnetometer (FGM) [Balogh *et al.*, 1997] and the ion spectrometer (CIS) [Reme *et al.*,

1997]. The Cluster spacecraft orbital plane precesses around the Earth annually. From 2001 to 2003 the Cluster spacecraft apogees were in the magnetotail between July and October. At apogee the spacecraft were in a nearly regular tetrahedron. In the magnetotail seasons of 2001 and 2002 the tetrahedron's spacing was 1000 km and 5000 km (i.e., on the order of the inertial range for turbulence within the plasma sheet), respectively. The latter spacing is ideal for examining turbulent eddy scale sizes that are on the order of 5000 to 20,000 km [Neagu *et al.*, 2002; Weygand *et al.*, 2005]. From July to October 2003, Cluster obtained another series of plasma sheet crossings at an interspacecraft spacing of about 100 km (i.e., on the order of dissipation range).

[15] Each Cluster spacecraft carries a boom-mounted triaxial fluxgate magnetometer [Balogh *et al.*, 1997]. Magnetic field vectors routinely are available at 22 Hz resolution (nominal mode). Both preflight and in-flight calibrations of the two magnetometers have been performed to produce carefully calibrated (and intercalibrated) magnetic field data. The relative uncertainty in the data after calibration is at most 0.1 nT, an estimate determined by examining the drift in the offset after calibration (K. K. Khurana and M. K. Schwarzl, private communication, 2004). The digital resolution of the magnetometer is on the order of 8 pT [Balogh *et al.*, 1997].

[16] The CIS instrument [Reme *et al.*, 1997] plays a key role in identifying periods when Cluster enters the PS, which is characterized by high electron and ion temperatures as well as significant H^+ , He^+ , and O^+ populations. CIS provides fundamental plasma parameters such as density, velocity vectors, pressure tensor, and heat flux. For this study the uncertainty in the density and temperature is not critical. In order to identify the plasma sheet we identify times when the values significantly increase or decrease and use periods when the density is greater than 0.1 ions cm^{-3} in order to identify when Cluster enters and exits the plasma sheet. The uncertainty of the velocity is approximately ± 2 km s^{-1} in the x and y components, but approximately ± 15 km s^{-1} in the z direction (L. M. Kistler, private communication, 2004). The V_z uncertainty was determined by assuming the mean V_z in the CPS is zero.

[17] The twin ACE magnetometer instruments measure the local interplanetary magnetic field direction and magnitude in the upstream solar wind at the first libration point. The triaxial fluxgate magnetometers are capable of a very wide dynamic range of measurements from ± 4 nT to $\pm 65,536$ nT per axis in eight discrete ranges with an uncertainty of about 0.025% in each range [Smith *et al.*, 1998]. These magnetometers have a temporal resolution of six vectors per second. The Solar Wind Electron, Proton, and Alpha Monitor (SWEPAM) measures the solar wind plasma electron and ion fluxes with separate sensors [McComas *et al.*, 1998]. Both sensors use electrostatic analyzers to provide plasma density, velocity, and thermal velocity measurements every 64 s.

[18] Cassini passed by the Earth in mid-August, 1999 on the way to Saturn. Data from the triaxial fluxgate magnetometer at about 32 Hz resolution are used in this study. These data have an uncertainty of about 0.1% in the gain and 0.1° in the pointing direction [Dougherty *et al.*, 2005].

[19] The IMP-8 spacecraft orbits the Earth in a near circular orbit at about 35 R_E with a spin rate of 24 rpm.

The magnetic field instrument (MAG) consists of a boom-mounted triaxial flux-gate magnetometer designed to study the interplanetary and geomagnetic tail magnetic fields. On 11 July 1975, because of a range indicator problem, the MAG experiment operation was frozen into the 36-nT range with 8 bit resolution. The digitization accuracy in this range is about ± 0.3 nT and the intrinsic sensor noise level is 0.03 nT RMS. See http://sd-www.jhuapl.edu/IMP/imp_merge_user_info.html for more information. The plasma data are obtained from the solar Faraday plasma cup (PLS). Measurements of the ion density, temperature, and flow are made once every 20 s. See ftp://space.mit.edu/pub/plasma/imp/fine_res for additional data.

[20] The Galileo spacecraft passed by the Earth twice while en route to Jupiter. For this study we used magnetic field measurements from the two triaxial fluxgate magnetometers. Data from the Earth flybys have a resolution of 5 Hz with an uncertainty of about ± 0.03 nT in the range of ± 512 nT common to the two sensor triads [Kivelson *et al.*, 1992].

[21] Like IMP-8, Geotail orbits close to the Earth with an apogee of about $30 R_E$ located in the solar wind during the summer months. Magnetic field data were obtained from the triaxial fluxgate magnetometer (MGF) with a resolution of about 3 s and an uncertainty of about ± 0.1 nT [Kokubun *et al.*, 1994]. Solar wind plasma flow vectors were measured by the low energy particle (LEP) experiment with a resolution of about 12 s [Mukai *et al.*, 1994].

[22] Our study used two instruments on the Wind spacecraft: the magnetometer (MFI) and the solar wind plasma instrument (3DP). The triaxial fluxgate magnetometers, mounted on a boom away from the spacecraft body, have a range ± 65536 nT and temporal resolution of 3 s [Lepping *et al.*, 1995] and provided IMF direction and magnitude. The Wind plasma instrument measures the solar wind ions and electrons with an energy resolution of $\Delta E/E$ of 0.2 [Lin *et al.*, 1995] and a temporal resolution of 3 s. This instrument was used to determine the solar wind speed.

3. Procedure

[23] In this section we outline the procedure used to construct the PDFs of magnetic field fluctuations with data from just one spacecraft or from two spacecraft and explain how we obtain the log-normal variance (λ) values from the Castaing *et al.* [1990] fit.

3.1. Single Spacecraft Probability Distribution Functions

[24] From single spacecraft measurements, one can construct the PDFs of temporal fluctuations of the magnetic field. In order to show that the PDFs from a single spacecraft are similar to those PDFs determined with two spacecraft PDFs, we require that the bulk flow be large enough such that the fluctuations change little in the time during which the plasma flows pass the spacecraft and we require that the bulk flow be in the solar ecliptic plane for study of the solar wind or in the geomagnetic ecliptic plane for study of the plasma sheet. The flow must be in the xy plane of these coordinate systems because the spacecraft in each region have the largest separations in the xy directions and relatively small separations in the z direction. The data

used to calculate the magnetic field fluctuations have been filtered with a Savitsky-Golay filter [Orfanidis, 1996] to remove the large-scale background features. The Savitsky-Golay filter fits a window of data around a point, for each point in the time series, with a fourth-order polynomial and removes the background field leaving the fluctuations. A procedure that removes slowly varying changes of the background field is especially important for plasma sheet data where the signature of the large-scale structure of the magnetotail dominates some of the magnetic field components. Once the data have been filtered we calculate the fluctuations over time τ in the i th component of the magnetic field from

$$\delta B_i(\tau, x) = B_i(t + \tau, x) - B_i(t, x). \quad (2)$$

The fluctuations are normalized to the standard deviation of the interval. PDFs are then constructed from the fluctuations and the PDF is fit with the Castaing *et al.* [1990] model (equation (1)) to obtain λ^2 . A reduced chi-square test was performed to determine the goodness of the fit. All the PDFs in this study were well fit with the Castaing *et al.* model. To establish whether non-self-similar scaling is present, we must determine how λ^2 varies with scale size.

3.2. Two Spacecraft Probability Distribution Functions

[25] The use of PDFs from single spacecraft measurements for tests of turbulence is based on an assumption that the fluctuations in the solar wind are frozen into the flow. If the assumption is valid, the results obtained from measurements of temporal fluctuations should not differ from those obtained by making two-point measurements, i.e., if the Taylor hypothesis applies, then PDFs of $\delta B_i(\tau, x)$ should be the same as PDFs of $\delta B_i(t, v_{\text{plasma}}\tau)$. Observations of the solar wind at separations of several hundred R_E demonstrate that this assumption is reasonable [Ridley, 2000]. Nonetheless, tests of the validity of using τ versus Δx have not been validated with measurements from multiple, spatially separated spacecraft. We can directly measure the fluctuations across space; however, we still need to assume that the fluctuations over the distances that we measure are manifestations of the same physical processes. This may be a reasonable assumption in the solar wind but may not always be the case within the plasma sheet. However, if we limit the analysis to intervals when the bulk flow is along the direction of the spacecraft separation, we think it likely that the underlying assumption is correct. After the application of the Savitsky-Golay filter, the magnetic field fluctuations are determined as

$$\delta B_i(\Delta x, t) = B_{2i}(x_1 + \Delta x, t) - B_{1i}(x_1, t) \quad (3)$$

where the scale Δx is a spatial separation between the two spacecraft and the first subscript on B identifies the spacecraft. From here the procedure is the same as that of section 3.1; PDFs of the normalized fluctuation are constructed and fit to obtain values for λ^2 , but this time for a range of spatial separations.

[26] To compare the results of the two procedures, the PDFs determined for temporal separations need to be mapped into the equivalent spatial separation PDFs. We assume that the Taylor hypothesis applies for the single spacecraft measurements and that time and space are related

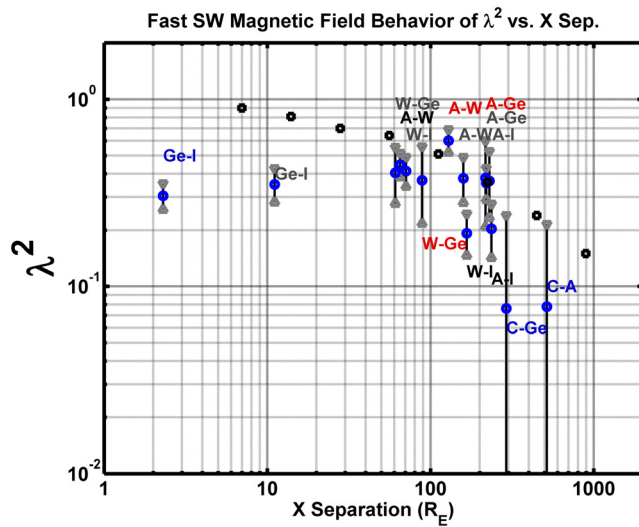


Figure 4. Scaling behavior of fast solar wind PDFs of magnetic field fluctuations. This figure has the same format as Figure 3.

(black text) 1998. We have assumed that the characteristics of the turbulent fluctuations in each interval are similar. Otherwise, we would not have a wide enough range of spatial separations to examine in each individual interval. Solar wind magnetic field measurements for the two periods in 1998 are based on data from four different spacecraft (ACE, Geotail, IMP-8, and Wind). We note that during the 12–21 June 1998 period three shocks pass the spacecraft. For comparison with results obtained by *Sorriso-Valvo et al.* [1999] (black squares), we related temporal to spatial separations using a solar wind speed of 420 km/s, which

is approximately the mean solar wind speed for a year's worth of data from 1998, and we adopted the Taylor hypothesis. The magnitudes and trends in λ^2 are similar despite the different intervals used.

[29] Figure 4 presents results for the fast solar wind and also indicates that the λ^2 of the log-normal variance (blue circles) decreases with increasing spatial separation. This plot used several fast solar wind periods: 19 August 1999 (Cassini Earth flyby with blue text); 27–30 August (gray text) 1999; 24–29 February (black text) 2000; and 10–14 November (red text) 2000. During the 24–29 February 2000 period one shock was observed. Again, the black squares are the results from *Sorriso-Valvo et al.* [1999] for the fast solar wind where we have assumed a solar wind speed of 550 km/s to obtain an equivalent spatial separation. Whereas the general trend in the data is for λ^2 to decrease with increasing Δx , the first two values of λ^2 do not follow the trend. We believe that our estimates of λ^2 based on the Geotail IMP-8 spacecraft pair in Figures 3 and 4 are low because of contributions from instrument noise. The magnetic field measured on Geotail has an uncertainty of 0.1 nT [Kokubun et al., 1994]. The magnetic field measured on IMP-8 has a quantization uncertainty of 0.3 nT (see http://sd-www.jhuapl.edu/IMP/imp_merge_user_info.html). The uncertainty in the Geotail magnetic field data is similar to that of data from most other solar wind spacecraft, but the uncertainty for IMP-8 (however, remarkable for a spacecraft that has supplied magnetic field data for about 27 years) is higher than average. Large-amplitude noise may dominate the ambient fluctuations and lead to a PDF that is more Gaussian than if the noise level were smaller.

[30] In Figure 5 we illustrate how adding a known amount of noise affects the PDFs and decreases the magnitude of the kurtosis. Shown in the top left panel of Figure 5

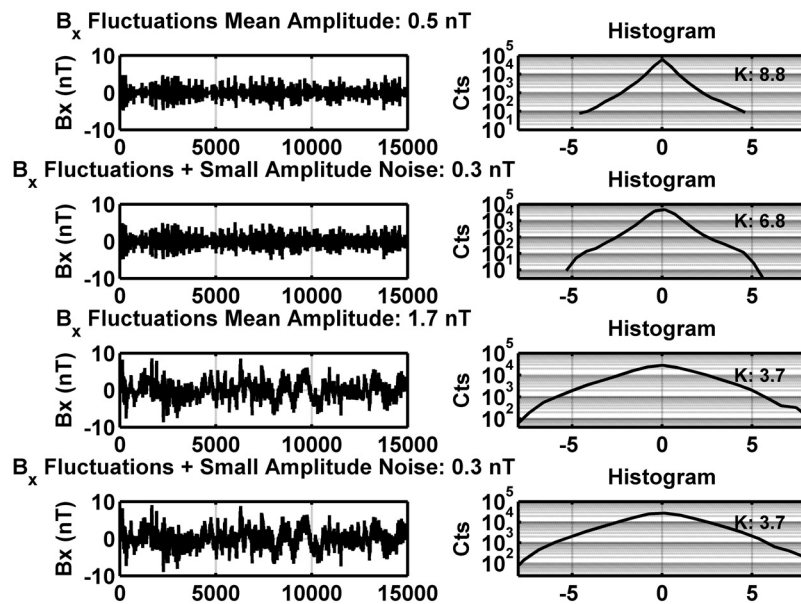


Figure 5. The effect of instrumental noise on the PDF shape and the kurtosis. These data were obtained from the ACE spacecraft. The column of panels on the left side has arbitrary units of time along the x axis. The title above each panel on the left gives the amplitude of the Gaussian distributed noise. The column of panels on the right side has units of counts on the y axis and the kurtosis is given in the upper right corner for each distribution.

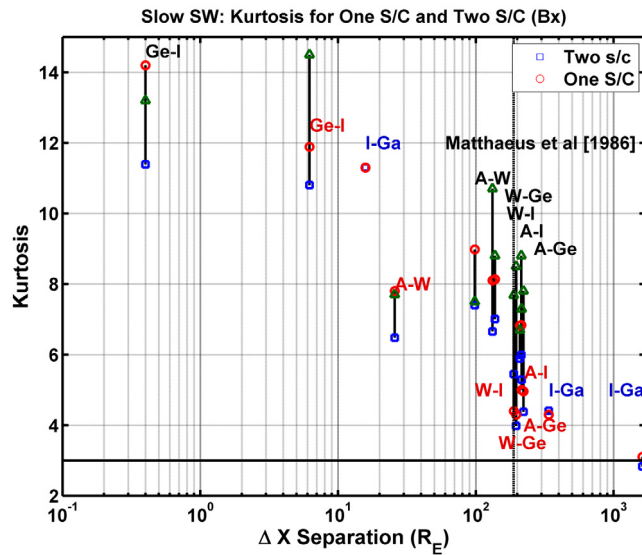


Figure 6. Kurtosis versus spatial separation determined from one (red circles) and two (blue squares) spacecraft PDFs of magnetic field fluctuations for slow solar wind. As in Figure 3, the letters identify the spacecraft pairs with the spacecraft used for the single spacecraft PDF given first. The vertical solid lines link the pairs of points determined from the two different methods. The vertical dashed line is placed at the minimum scale size of a turbulent solar wind eddy as determined by *Matthaeus et al.* [1986].

are the fluctuations of the B_x component, which have a mean amplitude of 0.5 nT, from the ACE measurements for a small temporal separation in the data. On the upper right is the normalized PDF of those fluctuations whose kurtosis is 8.8. The distribution has a sharp peak and resembles a double exponential distribution. The second row is the PDF from the same data with Gaussian distributed white noise with a standard deviation of 0.3 nT added to the fluctuations. This type of distribution of noise was added because it is the typical distribution for digitization noise, which is the dominant noise in the magnetometer (see http://sd-www.jhuapl.edu/IMP/imp_merge_user_info.html). The second row shows that the resulting PDF is more rounded at the peak and the kurtosis has decreased to 6.8 (i.e., a 22% decrease). The bottom two rows repeat the comparison with a large temporal separation in the data. In the third row the mean amplitude of the fluctuations is much larger and the PDF has a kurtosis of 3.7. In the bottom row the 0.3 nT noise has been added without affecting the kurtosis. From this simple experiment, we conclude that the larger amplitude digitization noise in the IMP-8 magnetometer decreases the value of the log-normal of the variance of the PDF at small temporal or spatial scale sizes, but does not affect the fluctuations when the scale size of the separation is large. This suggests that the two estimates of λ^2 for small separations in Figures 3 and 4 are underestimates, while the spacecraft pairs that use IMP-8 at large separations are not significantly affected.

[31] To summarize, we are able to reproduce the trends obtained by *Sorriso-Valvo et al.* [1999] and have obtained analogous results to their single spacecraft analysis with two

point measurements at different spatial separations over the range of spacings for which measurement limitations do not affect the analysis.

[32] Another approach to understanding the properties of the PDFs used to obtain Figures 1 to 4 is to establish the dependence of the kurtosis of the PDFs on Δx . The kurtosis indicates if the PDFs fall off slowly for large fluctuations. Figure 6 is a plot of the kurtosis versus spacecraft separation for the slow solar wind. The blue squares are the results for differences between two spacecraft and the red circles are determined from temporal fluctuations at one spacecraft, mapped from time into space as previously described. The black line joins points obtained by the two methods to assist the reader to compare values of the kurtosis. For each pair of points we have indicated which spacecraft pair was used to calculate the kurtosis; the first spacecraft in the pair is the one used for the single spacecraft measurements. A vertical black dashed line shows the *Matthaeus et al.* [1986] estimate of the minimum turbulent eddy scale size. Figure 7, for the fast solar wind, has the same format as Figure 6. In both figures the kurtosis decreases from some initial large value at small spacecraft separation to a value of about 3 for spacecraft separation of about 500 R_E . If the kurtosis of the fluctuation is thought to become 3 at spatial separations larger than a turbulent eddy scale size, then the 500 R_E length can be interpreted as roughly the scale size of the largest turbulent eddies. For both Figures 6 and 7 the mean difference between the kurtosis obtained from a single spacecraft or from the two point method is about 12% and the largest difference is 29%.

4.2. Plasma Sheet Probability Distribution Functions

[33] Figures 8 and 9 display the dependence of λ^2 on temporal and spatial separation of the magnetic field fluctuations in the plasma sheet. Local peaks in λ^2 are seen for time differences of about 0.03 and 0.086 hr (Figure 8),

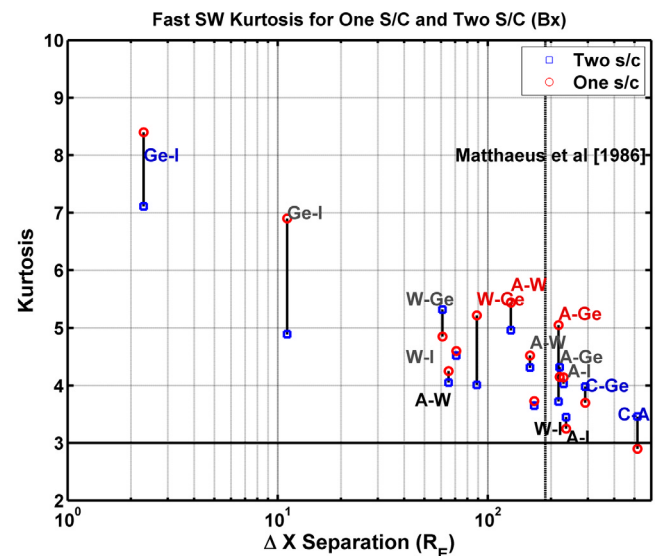


Figure 7. Kurtosis versus spatial separation determined from both one and two spacecraft PDFs of magnetic field fluctuations for fast solar wind. This figure has the same format as Figure 6.

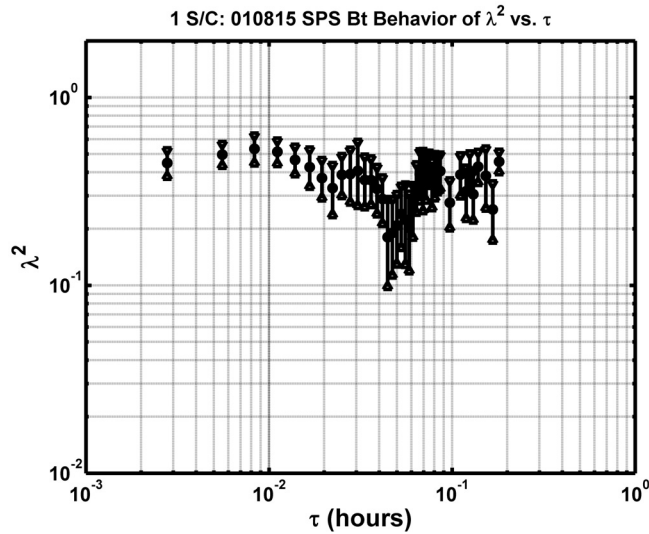


Figure 8. Scaling of PDFs observed in the plasma sheet for a range of temporal separation. This figure has the same format as Figure 1. These magnetic field fluctuations for this figure were recorded by Cluster on 15 August 2001 from 1013 UT to 1300 UT.

which corresponds to frequencies of 9.1 and 3.2 mHz. It is not clear what causes these peaks. *Kepko et al.* [2002] and *Walker* [2005] have suggested that density fluctuations in relatively narrow bands in the solar wind may excite characteristic frequencies of the magnetosphere at 1.3, 1.9, 2.6, and 3.3 mHz [*Samson et al.*, 1992] and it is possible that even lower frequency waves are intrinsic to the solar wind. This possibility needs further analysis. If the peaks are omitted, then the trend in the data is a decrease of λ^2 with increase of τ .

[34] The dependence of λ^2 on spatial separation is provided in Figure 9 for the limited range of two-spacecraft separations available from Cluster separations. The dashed vertical line in Figure 9 indicates the turbulent eddy scale size estimate according to *Neagu et al.* [2002], which was determined from the eddy turnover time and the RMS flow velocity in the manner introduced by *Borovsky et al.* [1997]. The events used for this figure are those for which the bulk plasma sheet flow is greater than 80 km/s in the X GSM direction. The requirement of a relatively high flow speed was motivated by a desire to measure turbulent fluctuations that arise from the same physical process in plasma with slowly changing coarse-scale bulk values of density and temperature. We have verified for the events in this study that the coarse-scale bulk properties vary slowly. We selected the flow speed of 80 km/s as low enough to result in acceptable statistics, but high enough for us to probe the spatial structure before it evolves significantly. The log-normal variance found for intervals of slower bulk plasma flow differs little from that of the higher flow speed intervals, but there is more scatter in the data.

[35] Figure 10 displays the kurtosis versus spatial separation for the plasma sheet magnetic field fluctuations using both one and two spacecraft data as previously described for the solar wind. Although the Taylor hypothesis most certainly does not apply under nominal plasma sheet condi-

tions, it should apply under plasma sheet conditions when the bulk flow is large and the Alfvén Mach number is greater than or close to 1. In the figure both the one spacecraft (triangles) and the two spacecraft (squares) kurtosis values show a decreasing trend over the full range of the measurements. The vertical dash-dot line is shown at the turbulent eddy scale size of about 5000 km estimated by *Neagu et al.* [2002] and the vertical dashed line at about 10,000 km is the estimated eddy scale size from *Borovsky et al.* [1997]. The mean difference between the one and two spacecraft kurtoses is about 32% and the maximum difference is about 70%.

5. *Hnat et al.* [2002] Analysis Method

[36] In this section we apply methods outlined by *Hnat et al.* [2002] as an additional means of identifying non-self-similar scaling. *Hnat et al.* [2002] show that the PDFs of solar wind fluctuations exhibit an approximately monofractal scaling law in the inertial range of 46 s to 26 hours using the functional form:

$$P(\delta B^2, \tau) = \tau^{-s} P_s(\delta B^2 \tau^{-s}, \tau) \quad (4)$$

where $\delta B^2 = B^2(t + \tau) - B^2(t)$, τ is the scale size (i.e., the temporal separation over which the magnetic field fluctuation is identified), and s is the constant scaling exponent. PDFs that satisfy the scaling relation given in equation (4) can be collapsed onto a single master curve. *Hnat et al.* [2002] showed that such a collapse is possible for magnetic fluctuations in the solar wind. If the scaling exponential is a constant and the PDFs collapse onto a single master curve, the fluctuations are monofractal. In the event that the PDFs are multifractal, *Hnat et al.* [2002] demonstrate that PDFs do not collapse to a single master curve but instead display

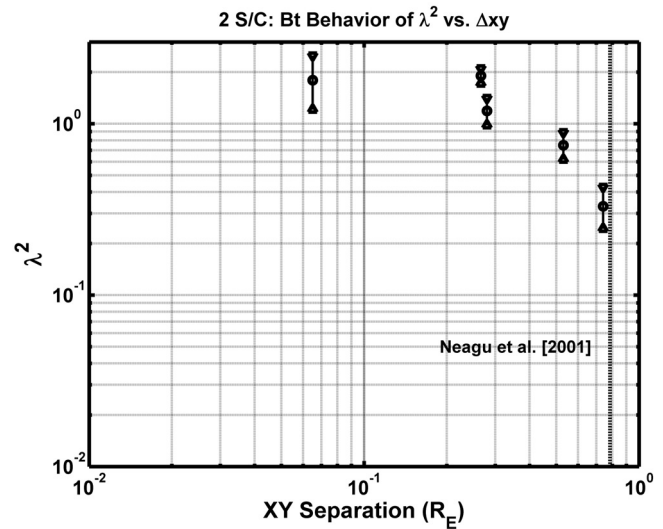


Figure 9. Scaling of PDFs for the plasma sheet over a range of spatial separations. This figure has the same format as Figure 3 and is a composite of several different events from 2001, 2002, and 2003. The vertical dashed line indicates the turbulent eddy scale size estimate from *Neagu et al.* [2002].

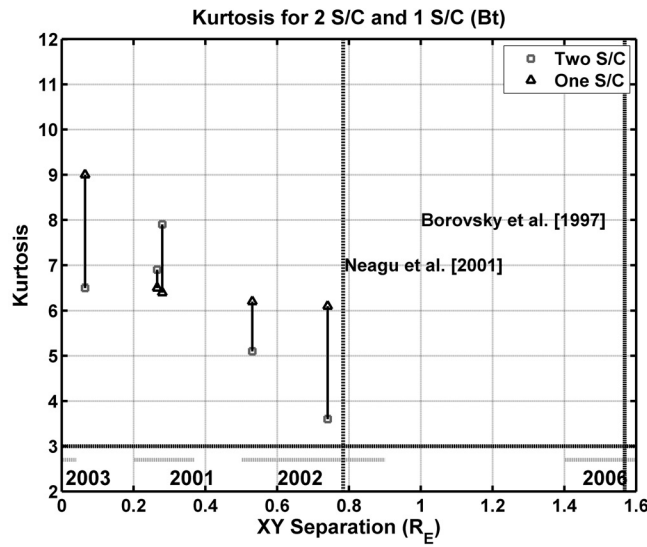


Figure 10. Variation of kurtosis versus spatial separation in the plasma sheet. This figure has the same format as Figure 6. The vertical dash-dot line is the turbulent eddy scale size in the plasma sheet estimated by *Neagu et al.* [2002] and the vertical dashed line is the turbulent eddy scale size estimated by *Borovsky et al.* [1997].

peaks with approximately the same height and wings whose height varies systematically with the scale size as shown in their Figure 5.

[37] As an intermediate step to rescaling the PDFs, *Hnat et al.* [2002] determine the scaling exponential by examin-

ing the log-log plot of the peak of the PDFs versus scale size for a range of scale sizes. Figure 3 in the *Hnat et al.* [2002] study demonstrates that, for self-similar scaling, the peak value of the PDF normalized to the area under the curve decreases linearly with increasing temporal scale. This figure shows that the scaling exponential is best described by a single constant. We have applied this procedure to the PDFs calculated using both the one and two spacecraft methods.

[38] Figure 11 displays log-log plots of the peak of the PDF versus a scale parameter, τ , for the PDFs calculated from a single spacecraft (Figures 11a and 11c) and that calculated from Δx for PDFs determined from two spacecraft (Figures 11b and 11d) for the solar wind (Figures 11a and 11b) and the plasma sheet (Figures 11c and 11d).

[39] The results differ for the one spacecraft PDFs and the two spacecraft PDFs. Several factors should be considered such as the spacecraft separations transverse to the flow direction, the use of combined intervals, and the effects of instrumental noise. If the spacecraft are not separated along the direction of the flow, or if the fronts are not aligned with normals along the flow direction, the actual temporal separation may differ from the temporal separation calculated from the mean separation and mean flow. When we restrict the solar wind spacecraft separations to $\leq 30 R_E$ (figure not shown) the scatter in Figure 11b is reduced, but the slope still differs from the one obtained in Figure 11a. A transverse separation of $30 R_E$ was adopted because the correlation between the two spacecraft begins to decrease significantly beyond this separation [*Richardson and Paularena*, 2001]. We also tried limiting the transverse separation for the plasma sheet analysis, but this process

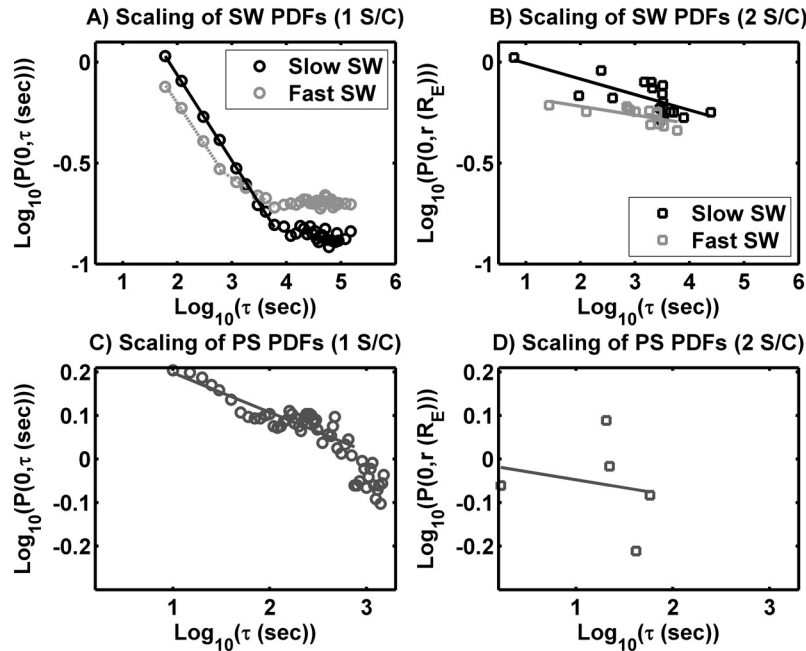


Figure 11. Log-log plots of the peak of the PDFs of the solar wind magnetic field fluctuations versus the scale size using the method of *Hnat et al.* [2002]. The top row uses solar wind measurements. The bottom row uses plasma sheet spacecraft. The left column gives results from single spacecraft PDFs; the right column gives results determined with pairs of spacecraft PDFs. The black points in Figure 11a are from intervals of slow solar wind and the grey points are from intervals of fast solar wind.

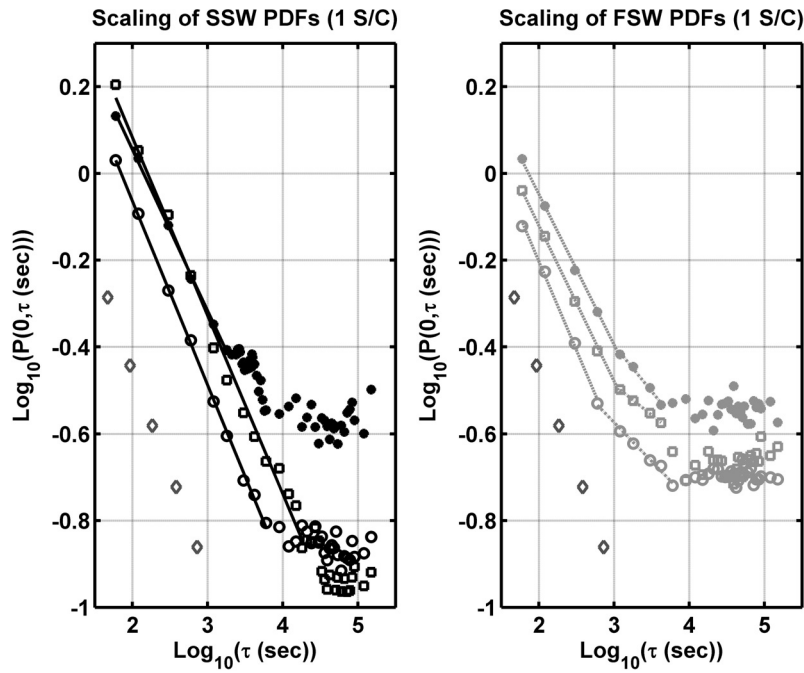


Figure 12. This figure has the same format as Figure 11. In the left panel are the points from three different slow solar wind periods. The circles apply to an interval in May 1998, the asterisks for November 1990, and the squares for June 1998. In the right panel is three different fast solar wind periods. The circles are for February 2000, the squares are for November 2000, and the asterisks are for August 1999. The slow solar wind periods show only one interval of self-similar scaling while the right panel shows two regions of self-similar scaling. In both panels the diamonds are the points taken from Figure 3 of *Hnat et al.* [2002].

reduces the data set to an unacceptably small number of measurements. An additional factor that may influence the values determined from spacecraft pairs is the fact that several different intervals of slow solar wind or of fast solar wind have been combined. Turbulence properties may differ in each interval and the combination of distinct intervals may affect the slope of the log-log plot. However, analysis of the individual solar wind intervals also gives results that differ from those in the top panels. Last, some of the scatter in the lower panels may result from the instrumental noise. As mentioned in the previous section, the use of multiple spacecraft adds noise to the fluctuations and for the IMP-8 spacecraft the uncertainty in the measurements is larger than the other spacecraft. Additional noise would reduce the height of the PDFs at small-scale sizes, similar to the decrease in the kurtosis of the PDFs, and could change the slope, but would not significantly affect the PDFs at large-scale sizes. Our best estimate is that the lack of agreement between the top and bottom plots results from a combination of all three factors discussed, but we require more events in order to test this hypothesis.

[40] While Figures 11a and 11b are not similar, Figure 11a resembles the relation reported by *Hnat et al.* [2002], especially for the slow solar wind. The most significant difference is the range over which a monofractal scaling (this down trending linear portion of the curve) applies. In *Hnat et al.* such scaling occurs between about 46 s and 26 hours, but the range in our interval extends from 1 min to about 100 min depending on the solar wind interval. Why there is a difference in the range is not clear. An additional

observable difference is the fast solar wind contains two regions of self-similar scaling as indicated by the break in the slope of the linear fit in the top left plot.

[41] Like the solar wind plots of Figure 11, the plasma sheet plots of the peak of the PDFs from a single spacecraft and from spacecraft pairs (Figures 11c and 11d) differ in form. The reasons for this are the same as those given for the solar wind. We also note that Figure 11c does not follow the same linear trend in the PDF peaks found in the equivalent solar wind plot. This is not unexpected because it has been found that the plasma sheet PDFs scale non-self-similarly [*Weygand et al.*, 2005], implying that the quantities plotted in Figures 11c and 11d should not follow a single linear trend, whereas the solar wind scale self-similarly [*Hnat et al.*, 2002] and should follow a linear trend in Figures 11a and 11b. Finally, we call to the reader's attention the peaks in Figure 11c between 100 and 1000 s. These peaks are believed to be real because the points that make up the peaks do not appear to be random and the peaks are observed in other log-log plots (not shown), not necessarily at the same temporal separations. These peaks will be discussed more fully in section 6.3.

[42] Figure 12 compares all individual slow and fast solar wind periods that we have examined to determine if monoscaling in the slow solar wind and biscaling in the fast solar wind are consistent features. The left panel compares three different slow solar wind regions and the right panel shows three different fast solar wind intervals. The diamonds in each figure are the values taken from Figure 3 of *Hnat et al.* [2002]. In the fast solar wind there are systematically two

Table 1. Table of the Scaling Exponentials Determined From Figure 12^a

| | First Scale Exp. | Second Scale Exp. |
|---------------------------|-------------------------------------|-----------------------------|
| <i>Hnat et al.</i> [2002] | -0.42 ± 0.02 (46 s to 26 hours) | |
| SSW 1990/11 (~3 days) | -0.37 (1 min to 30 min) | |
| SSW 1998/06 (~9 days) | -0.41 (1 min to 300 min) | |
| SSW 1998/05 (~8 days) | -0.42 (1 min to 102 min) | |
| FSW 2000/02 (~5 days) | -0.41 (1 min to 10 min) | -0.18 (10 min to 102 min) |
| FSW 2000/11 (~4 days) | -0.36 (1 min to 20 min) | -0.14 (20 min to 72 min) |
| FSW 1999/08 (~3 days) | -0.35 (1 min to 20 min) | -0.21 (20 min to 72 min) |

^aGiven in the left column is the type of solar wind (slow solar wind: SSW and fast solar wind: FSW) and the date of the intervals. In then second column is the value for the first scaling region plus the range over which the scaling applies. The far right column is the value for the second scaling exponential if it is applicable. The top row show s the value given by *Hnat et al.* [2002].

different scaling regions. The slow solar wind seems to show a single scaling region. The slow solar wind interval of November 1990 shows two small peaks at values of $\log_{10}(\tau)$ above 3.25 to 3.59. These peaks are similar to, but smaller than, the peaks observed in Figure 11c for the plasma sheet. Table 1 compares the scaling exponential for each of these periods and indicates that the first scaling exponential for each slow solar wind interval is close to the value calculated by *Hnat et al.* [2002], which is given in the top row of the table. The mean scaling exponential is about -0.4 , within the uncertainty given by *Hnat et al.* [2002]. Table 1 also shows that in the slow solar wind the break point of the self-similar scaling differs considerably for the three periods and ranges from about 0.5 hours to 5 hours. For the fast solar wind, the scaling exponentials for the two scaling ranges and the positions of the two break points differ little from one interval to another. Our hypothesis regarding the physical significance of the break points will be discussed further in the next section.

6. Discussion

[43] By examining temporal fluctuations of the magnetic field on a single spacecraft and comparing them with the fluctuations of the field measured simultaneously at two different positions, we have been able to investigate the validity of the Taylor hypothesis for studies of the solar wind and the plasma sheet. Comparing our results with those reported by other investigators for fluctuations in time, we have in some cases reached different conclusions or extended previous analysis. Here we attempt to account for the features of our work that differ from or extend those previously reported.

6.1. Scaling Parameters in the Solar Wind and the Plasma Sheet

[44] Following *Sorriso-Valvo et al.* [1999], we analyzed temporal variations of the magnetic field using data from Wind near 1 AU and formulated the scaling behavior in terms of the *Castaing et al.* [1990] parameter λ^2 introduced in equation (1). *Sorriso-Valvo et al.* used data from Helios acquired between 1 AU and 0.29 AU. We reproduced the trend of the *Sorriso-Valvo et al.* scaling (λ^2 versus τ in Figures 1 and 2), but found systematically lower values for the fast solar wind. It is possible that the shift results from the different nature of the two data sets. Our work used continuous intervals of uninterrupted fast (or slow) solar

wind, whereas *Sorriso-Valvo et al.* used a superposition of multiple fast (or slow) solar wind intervals and did not exclude localized events such as coronal mass ejections or current sheet crossings. It is also possible that solar wind conditions were more extreme in the interval that they used or that solar wind turbulence evolves as the plasma propagates from 0.29 AU to 1 AU. It is interesting to note that *Sorriso-Valvo et al.* found larger λ^2 values for the fast solar wind than the slow solar wind, whereas we found just the opposite. Why this is the case is not clear at this time.

[45] We have also applied the *Castaing et al.* [1990] formulation to the differences of the magnetic field measured simultaneously at pairs of solar wind spacecraft. The variation of λ^2 with spacecraft separation in radial distance from the Sun, Δx , followed the trend found by *Sorriso-Valvo et al.* [1999], $\tau = \Delta x/v_{sw}$. The points in the two-spacecraft study that did not correspond to the single spacecraft results could be understood as contaminated by noise in the (aging) IMP-8 magnetometer.

[46] The plasma sheet was investigated using the same types of analysis. For this plasma, as for the solar wind, a nonlinear decrease in the variance of the log-normal distribution was found over a large range of scale sizes (Figures 8 and 9). This nonlinear decrease is consistent with intermittent turbulence of the plasma sheet and with properties of non-self-similar scaling. These results are consistent with those previously reported for field fluctuations [*Weygand et al.*, 2005] and for flow fluctuations [*Borovsky et al.*, 1997, 2003; *Angelopoulos et al.*, 1999; *Petrakovich and Yermolaev*, 2002]. *Angelopoulos et al.* [1999] used two spacecraft (Geotail and Wind) to demonstrate intermittency in the plasma sheet flow. However, the present study is the first to use spacecraft at a range of separations to investigate both intermittency and scaling features of the plasma sheet plasma. In comparing the present work with that of *Weygand et al.* [2005], we found that plasma sheet properties obtained from analysis of single spacecraft data corresponded well with the results obtained from spacecraft pairs, provided that the sunward flow exceeded 80 km/s in the X GSM direction. Noting that the properties of plasma in different parts of the magnetotail (lobe, plasma sheet boundary layer, central plasma sheet) differ considerably, the question arises in any multispacecraft study whether both spacecraft are probing a single continuous plasma regime. We believe that by limiting the analysis to data from intervals of above-average flow speed, we select cases

in which both spacecraft are embedded in the same plasma regime.

[47] The form of the PDF is expected to become Gaussian at the eddy scale size. In the *Angelopoulos et al.* [1999] case, the PDF of the flow fluctuations remained non-Gaussian at separations as large as $4.8 R_E$, whereas *Borovsky et al.* [1997] and *Borovsky and Funsten* [2003], *Neagu et al.* [2002], *Weygand et al.* [2005], and the present study find turbulent eddy scale sizes that range from 5000 to 20,000 km. Possibly the plasma sheet was particularly thick in the *Angelopoulos et al.* event. Wind magnetic field B_z data in the *Angelopoulos et al.* shows a dipolarization at about 1100 UT and hence a substorm occurred and the tail was in the recovery phase for most of the interval, which means the plasma sheet was thicker than normal. *Weygand et al.* [2005] also showed that the turbulent eddies in the plasma sheet are stretched along the x axis and thinner along the z axis. Furthermore, *Thompson et al.* [2005] has shown that the plasma sheet can be as thick as $8\text{--}10 R_E$. Additional studies are clearly needed to test relationships between turbulence and plasma sheet thickness or other features of the plasma sheet that may dictate eddy scale size. Such studies would provide insight into the differing results in the multiple investigations.

6.2. Eddy Scale Size Inferred From the Kurtosis of the PDFs

[48] The characteristics of solar wind fluctuations can be quantified in terms of the kurtosis of the distribution [e.g., *Burlaga and Viñas*, 2004] as an alternative to an analysis in terms of the log normal variance, λ^2 . Our results for the variance of magnetic field fluctuations versus temporal or spatial separation support the conclusions of *Burlaga and Viñas* in showing that the kurtosis decreases with increasing separation, asymptoting to a value of ~ 3 , applicable to a Gaussian distribution. However, the limiting value for the *Burlaga and Viñas* study is reached at about 280 hours, which for a nominal solar wind speed of 400 km/s implies a spatial separation of $\sim 63,000 R_E$ whereas we find that the kurtosis approaches 3 at $\sim 500 R_E$ (see Figures 6 and 7). Our result is within a factor of 3 of the eddy scale size of $190 R_E$ determined by *Matthaeus et al.* [2005] and within the range of 190 to $4400 R_E$ reported by *Matthaeus et al.* [1986].

[49] It is unclear why the *Burlaga and Viñas* [2004] study found Gaussian distributions only at extremely large spatial scales. Their work does not separate fast and slow solar wind, but we find that for both portions of the solar wind, the kurtosis of 3 is attained at several hundred R_E . It is possible that the properties of flow and field fluctuations differ among events, but it is hard to imagine such extreme differences.

[50] From the kurtosis of the PDFs of variations of the magnetic field in the plasma sheet, we have inferred eddy scale sizes of $0.9\text{--}1.5 R_E$, consistent with sizes reported by *Weygand et al.* [2005]. Values of $0.8 R_E$ and $1.6 R_E$ have been found by *Neagu et al.* [2002] and *Borovsky et al.* [1997], respectively. The range in the size of the turbulent eddies suggest that external conditions may control the scale size of plasma sheet eddies. However, more work needs to be done to confirm this hypothesis.

6.3. Turbulence Analysis in Terms of Peak Values of PDFs

[51] Another approach to turbulence analysis is based on the method of *Hnat et al.* [2002] who characterized the fluctuations of various solar wind properties versus τ or Δx by looking for trends in the peak values of the PDFs of the fluctuations. A linear trend implies self-similar scaling. Our analysis of two intervals of slow solar wind in Figure 12 agrees with the *Hnat et al.* conclusion that self-similar scaling is present over a range of temporal or spatial separations and demonstrates that the scaling exponential changes little from one to another interval of slow solar wind. In one particular interval, though, there appear to be several peaks similar to those observed in the plasma sheet (Figure 11c). The nature and meaning of these peaks is unclear at this time. However, similar peaks appear to be present in some of the intervals examined in Figure 14 of the *Consolini et al.* [2005] study. In the slow solar wind intervals we also found variations in the upper cutoff of the range of temporal or spatial separations for which self-similar scaling applies. Our cutoffs varied between 0.5 hours and 5 hours and were all smaller than the 26 hour cutoff reported by *Hnat et al.* We believe that the differences between our results relate to selection criteria. We treated intervals of slow and fast solar wind separately and avoided structures such as CMEs, whereas *Hnat et al.* used several years of solar wind data including all solar wind conditions.

[52] For nominal solar wind speed, our cutoffs imply eddy scale sizes of 370, 110, and $1100 R_E$ for the three solar wind intervals that we investigated. These can be compared with the range of eddy scale sizes (190 to $4400 R_E$) reported by *Matthaeus et al.* [1986] and with the $190 R_E$ reported more recently by *Matthaeus et al.* [2005] who combined more than 100 solar wind intervals for their study. These variations of the cutoff scale suggest the possibility that the eddy scale size may change depending on properties of the coronal source of the solar wind, a proposal worthy of further investigation.

[53] In Figure 11 we compared the results for PDFs obtained from single spacecraft and pairs of spacecraft and observed little agreement between the plots. We attributed this lack of agreement to a combination of factors that include nonideal spacecraft alignment, noise in the data, and differences in the turbulent properties in each of the intervals.

6.4. Power Spectral Density Properties and Turbulence in the Solar Wind

[54] There is a long history of using power spectral density as a tool for identifying the properties of turbulent systems, the idea being that in regions of self-similar fluctuations, the power varies linearly with the frequency. The analyses described in the previous sections provided a cutoff in time whose inverse is expected to correspond to the low frequency end of the linear trend in the power spectrum. For the May 1998 slow solar wind intervals of our study (see Figure 13), we found the expected linear trend (corresponding to a slope of $-5/3$) over a range of frequencies starting slightly above the expected minimum value. For a second interval, November 1990, the cutoff in time at about 30 min did not correspond to a power density spectrum break at about $20 \mu\text{Hz}$ (power spectrum not

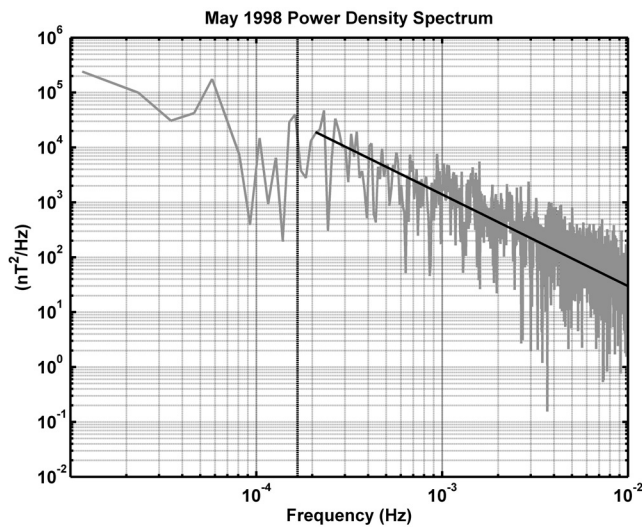


Figure 13. Power density spectrum for the slow solar wind period in May 1998. The black vertical dashed line marks the break observed in left panel of Figure 12 at about 6000 s. The solid black line is a linear fit to the data at approximately the break in the power density spectrum. The slope of this line is $-5/3$.

shown). Above $20 \mu\text{Hz}$ the spectral index is about -1.55 , which is near the Kraichnan [1965] estimated inertial range spectral index and a spectral index commonly observed in solar wind turbulence. The power spectra of the third interval did not reveal the same behavior due to the shortness of the interval and the low resolution of the data.

[55] For the fast solar wind (Figure 14), a break in the power spectral slope in the February 2000 interval corresponded to a frequency at which a break occurs within the log-log plot at about 10 min (about 1.67 mHz). The two break points (at about 1200 s and 4300 s) observed in the right plot of Figure 12 for the February 2000 fast solar wind event are plotted in Figure 14 at 1.67 and 0.16 mHz. At frequencies higher than the break point at 1.6 mHz the spectral index in the figure is about -1.5 . In between the break point at 0.167 mHz and 1.67 mHz the spectral index is about -1.0 , which is the spectral index commonly associated with the driving range of a turbulent power density spectrum [Goldstein *et al.* 1995]. The February 2000 interval was the only one of the three intervals examined in which the power spectra displayed breaks at the same periods as the log-log plots of Figure 12. The other two did not have enough high resolution data to enable us to find the breaks.

[56] As in the other approaches, the critical frequencies (or timescales) appear to vary by as much as an order of magnitude from one interval to another. The critical frequencies bound regions in which the power spectral density displays a linear decrease with frequency. This behavior is compatible with the behavior identified with other analysis techniques and suggests to us that the solar wind behaves in a self-similar manner over one or more ranges of temporal or spatial fluctuations but that the critical scale sizes can change from one portion of solar wind to another.

6.5. Isolated Spectral Peaks

[57] Several of our plots of properties of the magnetospheric plasma sheet (note especially Figures 8 and 11c) contain isolated points that depart from the trend. We have remarked that these anomalous points could be related to the “magic frequencies” of Samson *et al.* [1992]; see also Kepko *et al.* [2002] and Walker [2005]. In Figure 8 only one of the peaks at 3.3 mHz corresponds to one of the Samson *et al.* [1992] frequencies. The other peak at about 13.9 mHz is much larger than any of the Samson *et al.* frequencies but falls in the Pc 4 band that corresponds to magnetospheric field line resonances. In Figure 11c one of the peaks at about 2.1 mHz is close to the magic frequency of about 1.9 mHz, but none of the other peaks are similar to any of the other frequencies. The true nature of the peaks in Figures 8 and 11c is not clear. Additional intervals should be analyzed to compare peaks with the Samson *et al.* frequencies. It is clear in both figures that the plasma of the plasma sheet is non-self-similar over a large range of scale sizes.

6.6. Taylor Hypothesis

[58] It is widely accepted that the Taylor hypothesis applies in the solar wind. The use of both one and two spacecraft techniques in this study presents us with the opportunity to check this assumption. A comparison of Figures 1 and 2 with Figures 3 and 4 and the one and two spacecraft values of the kurtosis in Figures 6 and 7 show that similar values are obtained from spatial and temporal analysis. The results are consistent with the Taylor hypothesis. Differences between the two methods can be explained by either instrument noise or by the assumption that spacecraft did not probe a homogeneous regime. The

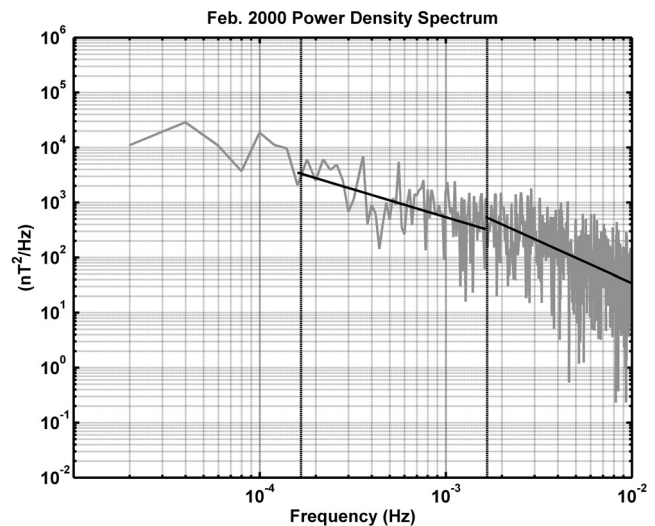


Figure 14. This figure has the same format as Figure 13, but for the fast solar wind interval in February 2000. At approximately 1.67 mHz there appears to be breaks in the power density spectrum. This break is close to the first break observed in the right panel of Figure 12 at 600s, which is marked with the right black vertical dashed line. The left vertical dashed line marks the second break observed in Figure 12 at about 6000 s.

mean difference between the kurtosis determined with a single spacecraft and the kurtosis determined with the spacecraft pairs is about 12% with a maximum difference of 29%.

[59] In the plasma sheet the Taylor hypothesis is most certainly not true under nominal conditions. However, under some conditions the Taylor hypothesis could apply. For intervals in which the bulk speed of the plasma is above average, the kurtoses calculated using the two different methods do not differ greatly (see Figure 10). The mean difference is about 32% and the largest difference is 70%. We recommend that additional studies be done in order to identify conditions for which the Taylor hypothesis begins to fail.

6.7. Is Solar Wind Turbulence Self-Similar?

[60] The analysis of this and other papers leads to conflicting conclusions on the question of whether turbulence in the solar wind is self-similar. Using the parameter λ^2 introduced by Castaing *et al.* [1990], we concluded that the solar wind has non-self-similar scaling properties over a large range of scale sizes. Using the approach of Hnat *et al.* [2002], we were led to similar conclusions for the fast solar wind and the plasma sheet but we obtained ambiguous results for the slow solar wind. Possibly the differences arise because of the analysis methods, but there may be underlying physical reasons for the different results obtained at this time. For example, the concepts that we apply to the description of turbulence were developed for the analysis of homogeneous systems characterized by fixed boundaries (such as the radius of an obstacle in a flow) but long intervals of the solar wind include portions with different scale sizes. If the characteristic eddy sizes differ not only between fast and slow solar wind but also among different intervals of slow or fast solar wind, the significance of the superposed PDFs may be ambiguous. Many of the properties of the solar wind are imposed in the solar corona. Particularly because of our evidence that the cutoff scales differ from one to another interval of slow solar wind, it seems quite plausible that features of the turbulence are imposed at the coronal source and that properties inferred from long intervals of solar wind data produce ambiguous results because they are inferred from data that superimposes parameters from distinct plasma regimes.

7. Summary and Conclusions

[61] We have applied several different methods of identifying self-similarity in the solar wind and plasma sheet. Both the Hnat *et al.* [2002] method and Sorriso-Valvo *et al.* [1999] method demonstrate that the fast solar wind and plasma sheet have non-self-similar scaling properties. In the slow solar wind our results are conflicting. The Sorriso-Valvo *et al.* [1999] method suggests that the slow solar wind has non-self-similar scaling properties, while the Hnat *et al.* [2002] method suggests that it has self-similar scaling properties.

[62] In addition to obtaining results similar to those of Sorriso-Valvo *et al.* [1999] and Hnat *et al.* [2002] studies, we used spacecraft pairs in both the solar wind and the plasma sheet to demonstrate that we are able to obtain results with spatially separated spacecraft that are similar to

those obtained from a single spacecraft. The fact that we are able to obtain analogous PDFs and kurtoses with both methods in the solar wind indicates that the Taylor hypothesis is a valid assumption in the solar wind and most likely applicable under specific conditions of above average flow in the plasma sheet.

[63] Furthermore, the PDFs of magnetic field fluctuations are non-Gaussian at scales smaller than about 500 R_E and 1.5 R_E in the solar wind and plasma sheet, respectively. The highly peaked shape with high probability wings (i.e., a distribution with a kurtosis >3) generally indicates that intermittent turbulence is present within the plasma.

[64] Finally, plots of the kurtosis versus spatial separation suggest that the turbulent eddy scale size for the slow and fast solar wind is about 500 R_E . This is consistent with the previous work of Matthaeus *et al.* [1986], but a factor of about 3 higher than their more recent work [Matthaeus *et al.* 2005]. In the plasma sheet we found that the turbulent eddy scale size was about 0.9 R_E for the spacecraft pairs but 1.5 R_E for the single spacecraft measurements. Both these values are consistent with the previous work of Weygand *et al.* [2005], but additional values from 2006 are required to refine the estimate.

[65] **Acknowledgments.** This work was supported by NASA grant NAG5-12131. We would also like to thank R. Silva for her assistance and S. Joy, C. Smith, J. Bieber, W. Matthaeus, R. Lepping, and B. Hnat for their advice.

[66] Wolfgang Baumjohann thanks Manfred Leubner and another reviewer for their assistance in evaluating this paper.

References

- Aellig, M. R., S. Hefti, H. Grünwaldt, P. Bochsler, P. Wurz, F. M. Ipavich, and D. Hovestadt (1999), The Fe/O elemental abundance ratio in the solar wind as observed with SOHO/CELIAS/CTOF, *J. Geophys. Res.*, **104**, 24,769.
- Angelopoulos, V., T. Mukai, and S. Kokubun (1999), Evidence of intermittency in Earth's plasma sheet and implications for self-organized criticality, *Phys. Plasmas*, **6**, 4161.
- Balogh, A., et al. (1997), The Cluster magnetic field investigation, *Space Sci. Rev.*, **79**, 65.
- Borovsky, J. E., R. C. Elphic, H. O. Funsten, and M. F. Thomsen (1997), The Earth's plasma sheet as a laboratory for turbulence in high-beta MHD, *J. Plasma Phys.*, **57**, 1.
- Borovsky, J. E., and H. O. Funsten (2003), The MHD turbulence in the Earth's plasma sheet: Dynamics, dissipation, and driving, *J. Geophys. Res.*, **108**(A7), 1284, doi:10.1029/2002JA009625.
- Burlaga, L. F., and A. F. Viñas (2004), Multiscale structure of the magnetic field and speed at 1 AU during the declining phase of solar cycle 23 described by a generalized Tsallis probability distribution function, *J. Geophys. Res.*, **109**, A12107, doi:10.1029/2004JA010763.
- Castaing, B., Y. Gagne, and E. J. Hopfinger (1990), Velocity probability distribution functions of high Reynolds number turbulence, *Physica D*, **46**, 177.
- Consolini, G., M. Kretschmar, A. T. Y. Lui, G. Zimbardo, and W. M. Macek (2005), On the magnetic field fluctuations during magnetospheric tail current disruption: A statistical approach, *J. Geophys. Res.*, **110**, A07202, doi:10.1029/2004JA010947.
- Dougherty, M. K., et al. (2005), Cassini Magnetometer Observations during Saturn orbit insertion, *Science*, **307**, 1266.
- Escoubet, C. P., R. Schmidt, and M. L. Goldstein (1997), Cluster-science and mission overview, *Space Sci. Rev.*, **79**, 11.
- Hnat, B., S. C. Chapman, G. Rowlands, N. W. Watkins, and W. M. Farrell (2002), Finite size scaling in the solar wind magnetic field energy density as seen by WIND, *Geophys. Res. Lett.*, **29**(10), 1446, doi:10.1029/2001GL014587.
- Hnat, B., S. C. Chapman, and G. Rowlands (2003), Intermittency, scaling, and Fokker-Plank approach to fluctuations of the solar wind bulk plasma parameters as seen by the WIND spacecraft, *Phys. Rev. E*, **67**, 056404.
- Goldstein, M. L., D. A. Roberts, and W. H. Matthaeus (1995), Magnetohydrodynamic turbulence in the solar wind, *Annu. Rev. Astron. Astrophys.*, **33**, 283.

- Kepko, L., H. E. Spence, and H. J. Singer (2002), ULF waves in the solar wind as direct drivers of magnetospheric pulsations, *Geophys. Res. Lett.*, **29**(8), 1197, doi:10.1029/2001GL014405.
- Kivelson, M. G., K. K. Khurana, J. D. Means, C. T. Russell, and R. C. Snare (1992), The Galileo magnetic field investigation, *Space Sci. Rev.*, **60**, 2357.
- Kokubun, S., T. Yamamoto, M. H. Acuña, K. Hayashi, K. Shiokawa, and H. Kawano (1994), The GEOTAIL magnetic field experiment, *J. Geomagn. Geoelectr.*, **46**, 7.
- Kolmogorov, A. N. (1941), The local structure of turbulence in incompressible viscous fluid for very large Reynolds' numbers, *Dokl. Akad. Nauk SSSR*, **30**, 301.
- Kraichnan, R. H. (1965), Inertial range of hydromagnetic turbulence, *Phys. Fluids*, **8**, 1385.
- Lepping, R. P., et al. (1995), The WIND magnetic field investigation, *Space Sci. Rev.*, **71**, 207.
- Leubner, M. P., and Z. Vörös (2005), A nonextensive entropy approach to solar wind intermittency, *Astrophys. J.*, **618**, 547.
- Lin, R. P., et al. (1995), A three-dimensional plasma and energetic particle investigation for the Wind spacecraft, *Space Sci. Rev.*, **71**, 125.
- Marsch, E., and C. Y. Tu (1994), Non-Gaussian probability distributions of the solar wind fluctuations, *Ann. Geophys.*, **12**, 1127.
- Matthaeus, W. H., M. L. Goldstein, and J. H. King (1986), An interplanetary magnetic field ensemble at 1 AU, *J. Geophys. Res.*, **91**, 59.
- Matthaeus, W. H., S. Dasso, J. M. Weygand, L. J. Milano, C. W. Smith, and M. G. Kivelson (2005), Spatial correlation of solar wind turbulence from two point measurements, *Phys. Rev. Lett.*, **95**, 231101.
- McComas, D. J., S. J. Bame, P. Barker, W. C. Feldman, J. L. Phillips, and P. Riley (1998), Solar wind electron proton alpha monitor (SWEPAM) for the Advanced Composition Explorer, *Space Sci. Rev.*, **86**, 563.
- Mukai, T., Y. Saito, M. Hirahara, T. Terasawa, N. Kaya, T. Obara, M. Ejiri, and A. Nishida (1994), The low energy particle (LEP) experiment on-board the GEOTAIL Satellite, *J. Geomagn. Geoelectr.*, **46**, 669.
- Neagu, E., J. E. Borovsky, M. F. Thomsen, S. P. Gary, W. Baumjohann, and R. A. Treumann (2002), Statistical survey of magnetic field and ion velocity fluctuations in the near-Earth plasma sheet Active Magnetospheric Particle Trace Explorers/Ion Release Module (AMPTE/IRM) measurements, *J. Geophys. Res.*, **107**(A7), 1098, doi:10.1029/2001JA000318.
- Orfanidis, S. J. (1996), *Introduction to Signal Processing*, Prentice-Hall, Englewood Cliffs, N. J.
- Petrukovich, A. A., and Y. L. Yermolaev (2002), Interball-tail observations of vertical plasma motions in the magnetotail, *Ann. Geophys.*, **20**, 321.
- Rème, H., et al. (1997), The Cluster ion spectrometry (CIS) experiment, *Space Sci. Rev.*, **79**, 303.
- Richardson, J. D., and K. I. Paularena (2001), Plasma and magnetic field correlations in the solar wind, *J. Geophys. Res.*, **106**, 239.
- Ridley, A. J. (2000), Estimation of the uncertainty in timing the relationship between magnetospheric and solar wind processes, *J. Atmos. Sol. Terr. Phys.*, **62**, 757.
- Samson, J. C., B. G. Harrold, J. M. Ruohoniemi, R. A. Greenwald, and A. D. M. Walker (1992), Field line resonances associated with MHD wave-guides in the magnetosphere, *Geophys. Res. Lett.*, **19**, 441.
- Smith, C. W., J. L. Heureux, N. F. Ness, M. H. Acuna, L. F. Burlaga, and J. Scheffele (1998), The ACE magnetic fields experiment, *Space Sci. Rev.*, **86**, 613.
- Sorriso-Valvo, L., V. Carbone, and P. Veltri (1999), Intermittency in the solar wind turbulence through probability distribution functions of fluctuations, *Geophys. Res. Lett.*, **26**, 1801.
- Sorriso-Valvo, L., V. Carbone, P. Giuliani, P. Veltri, R. Bruno, V. Antoni, and E. Martines (2001), Intermittency in plasma turbulence, *Planet. Space Sci.*, **49**, 1193.
- Thompson, S. M., M. G. Kivelson, K. K. Khurana, R. L. McPherron, J. M. Weygand, A. Balogh, H. Rème, and L. M. Kistler (2005), Dynamic Harris current sheet thickness from Cluster current density and plasma measurements, *J. Geophys. Res.*, **110**, A02212, doi:10.1029/2004JA010714.
- Vörös, Z., et al. (2003), Multi-scale magnetic field intermittence in the plasma sheet, *Ann. Geophys.*, **21**, 1955.
- Vörös, Z., W. Baumjohann, R. Nakamura, M. Volwerk, and T. L. Zhang (2004), Wavelet analysis of magnetic turbulence in the Earth's plasma sheet, *Phys. Plasmas*, **11**, 1333.
- Walker, A. D. M. (2005), *Magnetohydrodynamic Waves in Geospace: The Theory of ULF Waves and Their Interaction With Energetic Particles in the Solar-Terrestrial Environment*, Inst. of Phys. Publ., Bristol, U. K.
- Weygand, J. M., et al. (2005), Plasma sheet turbulence observed by Cluster II, *J. Geophys. Res.*, **110**, A01205, doi:10.1029/2004JA010581.

A. Balogh, Space and Atmospheric Physics Group, Physics Department, Blackett Laboratory, Prince Consort Road, London SW7 2BZ, UK.

M. L. Goldstein, NASA Goddard Space Flight Center, Code 612.2 Greenbelt, MD 20771, USA.

L. M. Kistler, Institute for the Study of Earth, Oceans, and Space, University of New Hampshire, 39 College Road, Durham, NH 03824, USA.

K. K. Khurana, M. G. Kivelson, H. K. Schwarzl, R. J. Walker, and J. M. Weygand, Institute of Geophysics and Planetary Physics, University of California, Los Angeles, 3845 Slichter Hall, P. O. Box 951567, Los Angeles, CA 90095-1567, USA. (jweygand@igpp.ucla.edu)